

EDITORS

of CUNY

Technology

Technology

an
nic Institute

bridge Research
homme
ty

Fluidization Engineering

SECOND EDITION

Daizo Kunii

Fukui Institute of Technology
Fukui City, Japan

Octave Levenspiel

Chemical Engineering Department
Oregon State University
Corvallis, Oregon

Butterworth-Heinemann

An Imprint of Elsevier

Boston London Singapore Sydney Toronto Wellington

Copyright © 1991 by Butterworth-Heinemann, a division of Reed Publishing (USA) Inc. All rights reserved.

No part of this publication may be reproduced, stored in a retrieval system, or transmitted, in any form or by any means, electronic, mechanical, photocopying, recording, or otherwise, without the prior written permission of the publisher.

Permissions may be sought directly from Elsevier's Science and Technology Rights Department in Oxford, UK. Phone: (44) 1865 843830, Fax: (44) 1865 853333, email: permissions@elsevier.co.uk. You may also complete your request on-line via the Elsevier homepage: <http://www.elsevier.com> by selecting "Customer Support" and then "Obtaining Permissions".

- ② Recognizing the importance of preserving what has been written, it is the policy of Butterworth-Heinemann to have the books it publishes printed on acid-free paper, and we exert our best efforts to that end.

Library of Congress Cataloging-in-Publication Data

Kunii, Daizo, 1923—
Fluidization engineering / Daizo Kunii, Octave Levenspiel.
—2nd ed.
p. cm.—(Butterworth-Heinemann series in chemical
engineering)
ISBN 0-409-90233-0
I. Fluidization. I. Levenspiel, Octave. II. Title.
III. Series.
TP156.F65K8 1991
660.2842—dc20
90-31800

British Library Cataloguing in Publication Data

Kunii, Daizo
Fluidization engineering.
1. Chemical engineering. Fluidisation
I. Title. II. Levenspiel, Octave
660.2842
ISBN 0-409-90233-0

Butterworth-Heinemann
313 Washington Street
Newton, MA 02158-1626

10 9 8 7

Contents

PREFACE TO THE SECOND EDITION	xvii
PREFACE TO THE FIRST EDITION	xix
NOTATION	xxi
CHAPTER 1 Introduction	1
The Phenomenon of Fluidization	1
Liquidlike Behavior of a Fluidized Bed	4
Comparison with Other Contacting Methods	7
Advantages and Disadvantages of Fluidized Beds for Industrial Operations	10
Fluidization Quality	11
Selection of a Contacting Mode for a Given Application	11
Overall Plan	12
Related Readings	13
CHAPTER 2 Industrial Applications of Fluidized Beds	15
Historical Highlights	15
Coal Gasification	15
Gasoline from Other Petroleum Fractions	15
Gasoline from Natural and Synthesis Gases	17
Synthesis Reactions	18
Metallurgical and Other Processes	18
Physical Operations	19
Heat Exchange	19
Solidification of a Melt to Make Granules	20

Coating Metal Objects with Plastic	20
Drying of Solids	21
Coating of Objects and Growth of Particles	23
Adsorption	24
Synthesis Reactions	27
Phthalic Anhydride	28
Fischer-Tropsch Synthesis	29
Acrylonitrile by the Sohio Process	31
Maleic Anhydride	33
Other Catalytic Reactions	33
Comments	34
Polymerization of Olefins	34
Cracking of Hydrocarbons	36
Fluid Catalytic Cracking (FCC)	36
Fluid Coking and Flexi-Coking	39
Thermal Cracking	40
Combustion and Incineration	42
Fluidized Combustion of Coal	42
Incineration of Solid Waste	44
Carbonization and Gasification	45
Gasification of Coal and Coke	45
Activation of Carbon	47
Gasification of Solid Waste	48
Calcination	49
Reactions Involving Solids	51
Roasting Sulfide Ores	51
Silicon for the Semiconductor and Solar	
Cell Industries	52
Chlorination and Fluorination of Metal Oxides	54
Reduction of Iron Oxide	55
Biofluidization	57
References	58
 CHAPTER 3	
Fluidization and Mapping of Regimes	61
Fixed Beds of Particles	61
Characterization of Particles	61
Fixed Beds—One Size of Particles	64
Fixed Beds—Solids with a Distribution of Sizes	65
Determination of the Effective Sphericity $\phi_{s,eff}$ from Experiment	67
<i>Example 1. Size Measure of Nonuniform Solids</i>	68
Fluidization without Carryover of Particles	68
Minimum Fluidizing Velocity, u_{mf}	68
Pressure Drop-versus-Velocity Diagram	71
Effect of Pressure and Temperature on Fluidized Behavior	74
Sintering and Agglomeration of Particles at High Temperature	75
<i>Example 2. Estimation of u_{mf}</i>	76

Types of Gas Fluidization without Carryover	76
The Geldart Classification of Particles	77
Fluidization with Carryover of Particles	80
Terminal Velocity of Particles, u_t	80
<i>Example 3. Estimate the Terminal Velocity of Falling Particles</i>	82
Turbulent and Churning Fluidization	83
Pneumatic Transport of Solids	84
Fast Fluidization	85
Voidage Diagrams for All Solid Carryover Regimes	87
The Mapping of Fluidization Regimes	88
<i>Example 4. Prediction of Flow Regime</i>	91
Problems	91
References	92
 The Dense Bed: Distributors, Gas Jets, and Pumping Power	
Distributor Types	95
Ideal Distributors	95
Perforated or Multiorifice Plates	96
Tuyeres and Caps	96
Pipe Grids and Spargers	97
Gas Entry Region of a Bed	98
Gas Jets in Fluidized Beds	101
Pressure Drop Requirements across Distributors	102
Design of Gas Distributors	105
<i>Example 1. Design of a Perforated Plate Distributor</i>	106
<i>Example 2. Design of a Tuyere Distributor</i>	108
Power Consumption	109
<i>Example 3. Power Requirement for a Fluidized Coal Combustor (FBC)</i>	110
Problems	111
References	112
 Bubbles in Dense Beds	
Single Rising Bubbles	115
Rise Rate of Bubbles	115
The Davidson Model for Gas Flow at Bubbles	116
Other Models for Gas Flow at Bubbles	120
Comparison of Models with Experiment	121
Evaluation of Models for Gas Flow at Bubbles	123
The Wake Region and the Movement of Solids at Bubbles	125
Solids within Bubbles	127
<i>Example 1. Characteristics of a Single Bubble</i>	129

Coalescence and Splitting of Bubbles	126
Interaction of Two Adjacent Bubbles	126
Coalescence, Bubble Size, and Bubble Frequency	127
Splitting of Bubbles and Maximum Bubble Size	129
Bubble Formation above a Distributor	130
<i>Example 2. Initial Bubble Size at a Distributor</i>	132
Slug Flow	132
Problems	134
References	134
CHAPTER 6	
Bubbling Fluidized Beds	137
Experimental Findings	137
Emulsion Movement for Small (Geldart B) and Fine (Geldart A) Particles	137
Emulsion Movement for Large (Geldart D) Particles	139
Emulsion Gas Flow and Voidage	141
Effect of Pressure on Bed Properties	141
Effect of Temperature on Bed Properties	142
Estimation of Bed Properties	143
Gas Flow in the Emulsion Phase	143
Bubble Gas Flow	143
Bubble Size and Bubble Growth	144
Bubble Rise Velocity	146
Beds with Internals	150
<i>Example 1. Bubble Size and Rise Velocity in Geldart A Beds</i>	150
<i>Example 2. Bubble Size and Rise Velocity in Geldart B Beds</i>	151
Physical Models: Scale-up and Scale-down	152
<i>Example 3. Scale-down of a Commercial Chlorinator</i>	153
Flow Models for Bubbling Beds	154
General Interrelationship among Bed Properties	155
The Simple Two-Phase Model	155
The K-L Model with Its Davidson Bubbles and Wakes	156
<i>Example 4. Reactor Scale-up for Geldart A Catalyst</i>	159
<i>Example 5. Reactor Scale-up for Geldart B Catalyst</i>	161
Problems	162
References	164
CHAPTER 7	
Entrainment and Elutriation from Fluidized Beds	165
Freeboard Behavior	165
Origin of Solids Ejected into the Freeboard	167

Experimental Findings	168
Location of the Gas Outlet of a Vessel	173
Estimation of the TDH	173
Entrainment from Tall Vessels: $H_f > \text{TDH}$	174
Procedure of Zenz et al. [21,8]	174
The Elutriation Constant Approach	175
Relationship between κ and G_s	176
Experimental Methods for Finding κ and κ^*	176
Experimental Findings for κ^*	177
<i>Example 1. Entrainment from Fine Particle Beds with High Freeboard</i>	179
<i>Example 2. Entrainment from Large Particle Beds with High Freeboard</i>	180
<i>Example 3. Entrainment from Beds with a Wide Size Distribution of Solids</i>	181
<i>Example 4. κ^* from Steady State Experiments</i>	181
<i>Example 5. Comparing Predictions for κ^*</i>	181
Entrainment from Short Vessels: $H_f < \text{TDH}$	183
Freeboard-Entrainment Model	184
<i>Example 6. Entrainment from a Short Vessel: $H_f < \text{TDH}$</i>	190
Problems	190
References	191
 CHAPTER 8 High-Velocity Fluidization	193
Turbulent Fluidized Beds	193
Experimental Findings	193
Fast Fluidization	195
Experimental Findings	197
The Freeboard-Entrainment Model Applied to Fast Fluidization	201
Design Considerations	203
Pressure Drop in Turbulent and Fast Fluidization	206
<i>Example 1. Performance of a Fast Fluidized Vessel</i>	206
Problems	209
References	209
 CHAPTER 9 Solid Movement: Mixing, Segregation, and Staging	211
Vertical Movement of Solids	212
Experimental Findings	212
Dispersion Model	214
Counterflow Solid Circulation Models	215
Relating the Counterflow to the Dispersion Model	216
Coarse Particle Beds	217
<i>Example 1. Vertical Movement of Solids</i>	218

Horizontal Movement of Solids	219
Experimental Findings	219
Mechanistic Model Based on the Davidson Bubble	220
<i>Example 2. Horizontal Drift of Solids</i>	222
Segregation of Particles	223
Mixing-Segregation Equilibrium	223
Steady State Separation of Particles	225
Large Solids in Beds of Smaller Particles	226
Large Solids Resting on Distributors	228
Staging of Fluidized Beds	228
Batch of Solids	228
Throughflow of Solids	231
Leakage of Solids through Distributor Plates	231
<i>Example 3. Design of Baffle Plates</i>	232
Problems	232
References	233
 CHAPTER 10	
Gas Dispersion and Gas Interchange in Bubbling Beds	237
Dispersion of Gas in Beds	237
Steady State Tracer Studies	237
Stimulus-Response Studies	242
Gas Interchange between Bubble and Emulsion	245
Definitions of Gas Interchange	245
Experimental Methods	246
Experimental Findings on Interchange Coefficients	248
Estimation of Gas Interchange Coefficients	250
<i>Example 1. Estimate Interchange Coefficients in Bubbling Beds</i>	253
<i>Example 2. Compare the Relative Importance of K_{bc} and K_{ce}</i>	254
<i>Example 3. Compare Interchange Rates for Adsorbed and Nonadsorbed Gases</i>	255
Problem	255
References	256
 CHAPTER 11	
Particle-to-Gas Mass and Heat Transfer	257
Mass Transfer: Experimental	257
Single Spheres and Fixed Beds	257
Gas Fluidized Beds	258
Interpretation of Mass Transfer Coefficients	259
Mass Transfer Rate from the Bubbling Bed Model	260
Effect of Adsorption on the Interchange Coefficient K _d	263

219	<i>Example 1. Fitting Reported Mass Transfer Data with the Bubbling Bed Model</i>	265
219	<i>Example 2. The Effect of m on Bubble-Emulsion Interchange</i>	267
220	Heat Transfer: Experimental	268
222	Single Spheres and Fixed Beds	268
223	Gas Fluidized Beds	268
225	Interpretation of Heat Transfer Coefficients	270
226	Attempt at Measuring h_p Directly in Fine Particle Beds	271
228	Heat Transfer from the Bubbling Bed Model	271
228	<i>Example 3. Fitting Reported Heat Transfer Data with the Bubbling Bed Model</i>	273
231	<i>Example 4. Heating a Particle in a Fluidized Bed</i>	274
232	Problems	275
232	References	276
37	CHAPTER 12 Conversion of Gas in Catalytic Reactions 277	
37	Measures of Reaction Rate and Reactor Performance	277
37	Previous Findings	278
42	Experimental Investigations	278
42	Reactor Models	284
45	Models for Complex Reactions	285
45	Multiple Stability	286
46	Design and Scale-up Procedures	288
48	Reactor Model for Fine Particle Bubbling Beds	289
48	First-Order Reaction	290
50	Special Cases of the Conversion Equation	292
53	Conversion Efficiency Compared to Plug Flow	293
54	<i>Example 1. Fine Particle (Geldart A) Bubbling Bed Reactor</i>	293
54	Application to Multiple Reactions	294
55	<i>Example 2. Commercial-Sized Phthalic Anhydride Reactor</i>	298
55	Reactor Model for Bubbling Beds of Intermediate-Sized Particles or	300
56	$u_{mf}/\epsilon_{mf} < u_b < 5u_{mf}/\epsilon_{mf}$	300
57	<i>Example 3. Bubbling Bed Reactor for Intermediate-Sized Particles</i>	302
57	Reactor Model for Large Particle Bubbling Beds	303
58	<i>Example 4. Reaction in the Slow Bubble Regime</i>	305
59	Reactor Model for the Freeboard Region above Fluidized Beds	305
60	<i>Example 5. Conversion in the Freeboard of a Reactor</i>	307
63	Turbulent Bed Reactors	308

Fast Fluidized Bed Reactors	309
Problems	309
References	310
CHAPTER 13 Heat Transfer between Fluidized Beds and Surfaces	313
Experimental Findings	313
Heat Transfer Coefficient	313
Vertical Tubes and Bed Walls	314
Horizontal Tubes	314
Splash Zone	317
Temperature Effect	317
Objects Immersed in Bubbling Beds	318
Fast Fluidized and Solid Circulation Systems	320
Radiant Heat Transfer	320
Heat Transfer Properties of Incipiently Fluidized Beds	322
Heat Transfer at a Distributor Plate	323
Theoretical Studies	323
Fixed and Incipiently Fluidized Beds	323
Bubbling Beds—Heat Transfer to Emulsion Packets	326
Bubbling Beds— h at a Heat Exchanger Surface h between Moving Beds and Heat Exchange Walls	328
Freeboard Region, Fast Fluidization, and Circulating Solid Systems	330
<i>Example 1. h on a Horizontal Tube Bank</i>	331
<i>Example 2. Effect of Gas Properties on h</i>	332
<i>Example 3. Effect of Particle Size on h</i>	332
<i>Example 4. Freeboard Heat Exchange</i>	334
Problems	334
References	335
CHAPTER 14 The RTD and Size Distribution of Solids in Fluidized Beds	337
Particles of Unchanging Size	337
Feed of One Size, Single and Multistage Beds	337
Feed of Wide Size Distribution	340
Simple Extensions	342
<i>Example 1. Flow with Elutriation</i>	343
<i>Example 2. Flow with Elutriation and Change in Density of Solids</i>	344
Particles of Changing Size	345
Rate Expressions for Growing and Shrinking Particles	345
General Performance Equations	346
Calculation Procedure for the General Situation	347

Linear Shrinkage, Single-Size Feed, No Elutriation	349
Linear Growth, Single-Size Feed, No Elutriation	350
Comments and Limitations	351
<i>Example 3. Single-Size Feed of Shrinking Particles</i>	351
<i>Example 4. Wide Size Distribution of Shrinking Particles</i>	352
<i>Example 5. Elutriation and Attrition of Catalyst</i>	353
Problems	356
References	357
 CHAPTER 15 Circulation Systems 359	
Circuits for the Circulation of Solids	359
Classification of Circulation Loops	359
Pressure Balance in a Circulation Loop	361
Finding Required Circulation Rates	365
Circulation Rate for Deactivating Catalysts	365
Circulation Rate for a Required Heat Removal Rate	367
<i>Example 1. Circulation Rate When Deactivation Controls</i>	369
<i>Example 2. Circulation Rate When Heat Duty Controls</i>	369
Flow of Gas-Solid Mixtures in Downcomers	371
Downward Discharge from a Vertical Pipe	373
Moving Bed Downflow	374
Fluidized Downflow	375
Fluidized Downflow in Tall Downcomers	376
Comments on Downcomers	377
<i>Example 3. Aeration of a Fine Particle Downcomer</i>	379
<i>Example 4. Circulation in Side-by-Side Beds</i>	380
<i>Example 5. Steam Seal of a Coarse Particle Downcomer</i>	381
Flow in Pneumatic Transport Lines	383
Vertical Uptake of Solids	383
Horizontal Flow	384
Safe Gas Velocity for Pneumatic Transport	385
Pressure Drop in Pneumatic Transport	385
Pressure Drop in Bends	388
Practical Considerations	388
Problems	392
References	394
 CHAPTER 16 Design for Physical Operations 397	
Information Needed for Design	397
Heat Transfer	398

CONTENTS

Batch Operations	398
Continuous Operations	400
Heat Loss to Surroundings	403
<i>Example 1. Single-Stage Limestone Calciner</i>	404
<i>Example 2. Multistage Limestone Calciner</i>	405
Mass Transfer	408
Batch Operations	408
Continuous Operations	410
<i>Example 3. Multistage Adsorber</i>	413
Drying of Solids	415
Batch Operations	415
Continuous Operations	418
<i>Example 4. Dryer Kinetics and Scale-up</i>	422
<i>Example 5. Solvent Recovery from Polymer Particles</i>	423
Problems	426
References	427
 CHAPTER 17	
Design of Catalytic Reactors	429
Bench-Scale Reactors	429
Pilot-Plant Reactors	430
Design Decisions	431
<i>Example 1. Reactor Development Program</i>	434
<i>Example 2. Design of a Commercial Acrylonitrile Reactor</i>	438
Deactivating Catalysts	440
<i>Example 3. Reactor-Regenerator with Circulating Catalyst: Catalytic Cracking</i>	444
<i>Catalytic Cracking</i>	447
Problems	448
References	
 CHAPTER 18	
The Design of Noncatalytic Gas-Solid Reactors	449
Kinetic Models for the Conversion of Solids	450
Uniform-Reaction Model for Porous Solids of Unchanging Size	450
Shrinking-Core Model for Solids of Unchanging Size	451
Intermediate Models for Particles of Unchanging Size	453
Models for Shrinking Particles	454
Finding the Right Model	455
Models for the Reaction of Solids Alone	456
<i>Example 1. Kinetics of Zinc Blende Roasting</i>	456
<i>Example 2. Kinetics of Carbon Burning</i>	457
Conversion of Solids of Unchanging Size	457
Single-Size Particles and Single Fluidized Bed	457

AUT
SUB

98	Single-Size Particles and Multiple Fluidized Beds	459
99	Size Distribution of Particles in a Single Bed	460
00	Remarks	461
03	<i>Example 3. Roasting Kinetics from Flowing Solids Data</i>	462
04	<i>Example 4. Scale-up of a Reactor with Flowing Solids</i>	462
05	Conversion of Shrinking and Growing Particles	464
08	Conversion of Both Gas and Solids	464
10	Performance Calculations for the Large Particle Bed (Case Z)	466
13	Performance Calculations for the Fine Particle Bed (Case W)	467
15	<i>Example 5. Design of a Roaster for Finely Ground Ore</i>	468
18	<i>Example 6. Design of a Roaster for Coarse Ore</i>	471
22	Miscellaneous Extensions	473
23	Wide Size Distribution of a Batch of Particles	473
26	Wide Size Distribution of Feed Solids to a Fluidized Bed	473
27	Fluidized Coal Combustion	474
29	Reactor-Regenerator System for Solids of Changing Size	476
30	Problems	476
31	References	479
34	AUTHOR INDEX	481
38	SUBJECT INDEX	487

, in *Fluidization*
153, Engineer
S. Satija and L.
59 (1985); K.D.
Fan, in *Circulat-*
P. Basu, ed., p.

g *Fluidized Bed*
Pergamon, New
Østergaard and
Engineering Founda-

on IV, D. Kunii
Engineering Founda-
E Symp. Ser.,
117 (1984); in
and A. Srensen,
ation, New York,

unication, 1985.
e, in *Circulating*
su, ed., p. 409,

Fluidized Bed
13, Compiegne,
g. Chem. Eng.,

d World Cong.

tion, City Uni-

chnology, D.L.

re, Washington,

at Soc. Chem.

1987.

g *Fluidized Bed*

59, Compiegne,

CHAPTER

9

Solid Movement: Mixing, Segregation, and Staging

- Vertical Movement of Solids
- Horizontal Movement of Solids
- Segregation of Particles
- Large Solids in Beds of Smaller Particles
- Staging of Fluidized Beds
- Leakage of Solid through Distributor Plates

As shown in Chap. 6 the channeling of the rising gas bubbles causes the gross circulation of solids in a fluidized bed, while the small-scale intermixing of particles occurs mainly within the wakes that accompany the bubbles up the bed. When solids of wide size distribution and/or of different densities are fluidized, the larger or heavier particles tend to settle to the bottom of bed, but this is countered by the solid circulation, mentioned above. At several multiples of u_{mf} of the largest or heaviest particles, the mixing process dominates. However, as the gas velocity is reduced to and then below u_{mf} of the largest or heaviest particles, these solids progressively concentrate at the bottom of the bed. Thus mixing and segregation of different solids is apparently an equilibrium process that depends on bed conditions. Since vertical segregation of different solids is absent in high-velocity fluidization typical of fast fluidization or pneumatic transport, this chapter only concerns bubbling and turbulent beds wherein u_o is close to u_{mf} of at least some of the bed solids.

The rate of horizontal mixing of solids is also of concern. This is especially so in long shallow beds wherein solids are fed at one end of the bed, react in the bed, and then leave at the other end of the bed.

Overall, there are numerous aspects to the mixing and movement of solids in fluidized beds. In this chapter we consider

- Vertical mixing and segregation of solids
- Horizontal mixing and dispersion of solids
- Mixing-segregation equilibrium
- Large solids in beds of small particles
- Transfer of solids across horizontal baffle plates and leaking through distributor plates

For the design of a number of physical and chemical processes it is important to understand the mechanism and rates of these opposing phenomena of mixing and segregation and related phenomena. In some situations one may even take

advantage of and deliberately encourage segregation of solids in the development of improved processes.

Vertical Movement of Solids

In catalytic reactors the large-scale vertical movement of porous particles can carry large amounts of adsorbed reaction components up and down the bed. This type of gas back mixing usually lowers conversion and selectivity. This is one reason why we need to know how much mixing of solids does occur, how to model this mathematically for predictive purposes, and what means are available to depress this movement.

As mentioned in Chap. 2, one often finds vertical or horizontal tubes fitted in catalytic reactors. These are placed there for various reasons: for temperature control, to reduce gulf circulation of solids, to reduce bubble size, to increase the emulsion voidage and thereby increase the overall residence time of reactant gas in the bed. All this raises the conversion of reactant gas and improves the selectivity of the desired product. For this reason various groups have also studied the movement of solids in beds with internals.

Experimental Findings

A variety of techniques have been used to study the vertical moment of solids, for example:

- Following the paths of individual tagged particles for long periods of time as they move about the bed.
- Measuring the extent of intermixing of two kinds of solids, originally located one above the other in the bed.
- Measuring the vertical spread of a thin horizontal slice of tracer solid.
- Finding the residence time distribution of the flowing stream in a bed with a throughflow of solids, using a variety of tracer techniques, such as step or pulse injection.
- Measuring the axial heat flow in a bed with a heated top section and cooled bottom section. This technique assumes that heat transport is caused solely by the movement of solids.

Surveys of the results of these many experimental studies are given by Kunii and Levenspiel [1], Potter [2], and van Deemter [3] in 1969, 1971, and 1985, respectively. These findings are most often reported in terms of the vertical dispersion coefficient D_{sv} . We briefly summarize them.

Beds without Internals. Figure 1(a) shows that the vertical mixing rate in rather small beds is directly related to the gas velocity by

$$D_{sv} = 0.06 + 0.1u_o , \quad [\text{m}^2/\text{s}] \quad (1)$$

and Fig. 1(b) shows that the vertical mixing of solids is more rapid in large-diameter beds than in smaller beds, the relationship being given by

$$D_{sv} = 0.30d_t^{0.65} , \quad [\text{m}^2/\text{s}] \quad (2)$$

In fact, in large vigorously bubbling fluidized beds of fine solids, the vertical movement of solids is very rapid. As an example, May [4] found that a slug

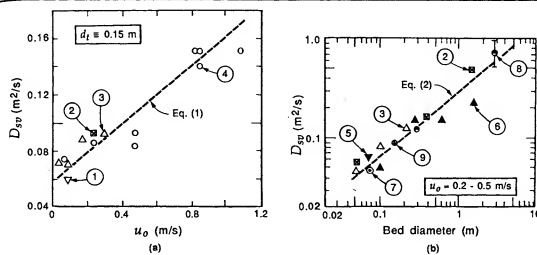


FIGURE 1

Vertical dispersion of solids in fine particle fluidized beds; from Avidan and Yerushalmi [5]; data from de Vries et al. [6] are added, and correlation line is modified somewhat from the original. (1) Stemmerding (Reman, 1955) [7], (2) May (1959) [4], (3) Thiel and Potter (1978) [8], (4) Avidan and Yerushalmi (1985) [5], (5) Lewis et al. (1962) [9], (6) de Groot (1967) [10], (7) Miyachi et al. (1968) [11], (8) de Vries et al. (1972) [6], (9) Avidan (1985) [5].

tracer introduced at one location in a large bed ($d_t = 1.52$ m, $L_f = 9.75$ m) of FCC catalyst became uniformly distributed throughout the bed in about 1 min.

Miyachi et al. [12] studied the vertical mixing of solids in vigorously fluidized ($u_o > 10$ cm/s) beds of fine Geldart A solids. Recall from Chap. 3 that in such beds bubbles quickly reach a small limiting size. They found that the mixing data could reasonably be represented by the dispersion model with

$$D_{sv} = 12u_o^{1/2}d_t^{0.9}, \quad [\text{cm}^2/\text{s}] \quad (3)$$

Example 1 compares values from this equation with the experimental values reported by de Groot [10].

Unfortunately, the dispersion model does not always well represent the vertical movement of solids. For example, May [4] found that for Geldart A solids the model well fitted the solid movement in his bed of aspect ratio $L_f/d_t = 9.1\text{ m}/0.38\text{ m} = 24$, but was inadequate for this bed of aspect ratio $L_f/d_t = 9.75\text{ m}/1.52\text{ m} = 6.4$.

Similarly, Avidan and Yerushalmi [5] found that the dispersion model well represented the mixing during turbulent fluidization where the bed looked close to homogeneous, but fitted the data poorly when the bed was in the bubbling regime.

To summarize, one may expect the dispersion model to reasonably represent the vertical mixing in tall beds in which rather small-scale mixing is taking place. This is characteristic of fine particle (Geldart A) systems with only mild gulf streaming. We would not expect it to satisfactorily represent shallow beds, beds with strong solid circulation, or beds with nonuniformly distributed internals.

Where the dispersion model does not fit well (gently bubbling and in not

very deep beds), the countercurrent mixing model often is used. This model views the solids moving in two streams, one rising and the other descending, with a crossflow or interchange between streams. This model closely matches the K-L model of Chap. 6 and is taken up in the next section.

Although the dispersion model does not reasonably represent the movement of solids in certain conditions, the results of experiments are invariably forced into this form and are reported in terms of a dispersion coefficient.

Beds with Internals. So far we have presented the findings on solid movement in beds free of internals. However, the presence of internals in a bed strongly hinders this movement. For example, Chen et al. [13] reported the following velocities of solids in the core of the upper vortex (refer to Fig. 6.3(d)) of their experimental bed containing horizontal tubes:

	No tube bundle in bed	Sparse bundle	Dense bundle
Average upward solid velocity (m/s) { at $u_o/u_{mf} = 4$ at $u_o/u_{mf} = 6$	0.19 0.26	0.09 0.15	0.01 0.02

Admittedly the bed was rather small ($d_t = 0.19$ m, $L_f \approx d_t$); however, these findings should indicate the general effect of bed internals.

In experiments with larger Geldart B solids in a 1.2×1.2 m bed that contained internals, Sitnai [14] noted that if a tube bank was located away from the wall of the bed, then solids would slide down in a thick stream along the wall surface, thereby generating a severe solid circulation pattern. So, to achieve a uniform solid movement, one should take this into account.

As an extreme of bed internals, Claus et al. [15] reported on the behavior of a fluidized bed ($d_t = 9.2$ cm, $L_m = 9.2$ m) packed with 2-cm wire screen Raschig rings. With Geldart B solids they found remarkably uniform fluidization with small bubbles throughout the bed. However, with fine Geldart A solids, fluidization was unsatisfactory, with considerable agglomeration of fine solids on the packing.

We next discuss the various models that have been used to interpret the experimental findings on the vertical moment of solids.

Dispersion Model

The *dispersion model* is a diffusion-type model represented by the differential equation

$$\frac{\partial C_s}{\partial t} = D_{sv} \frac{\partial^2 C_s}{\partial z^2} \quad (4)$$

where C_s is the concentration of tagged particles at position z at time t , and D_{sv} is the vertical dispersion coefficient averaged over the entire cross section of the bed.

The solution of Eq. (4) may take several forms. For a step input of tracer introduced into the stream of solids entering the bottom of a fluidized bed and leaving at the top, or vice versa, the use of the appropriate boundary and initial

This model
descending,
ly matches
the move-
invariably
ficient.

s on solid
ls in a bed
ported the
Fig. 6.3(d)

Dense
bundle

0.01
0.02

ever, these
n bed that
away from
ng the wall
achieve a

e behavior
ire screen
fluidization
t A solids,
e solids on
erpret the

differential

(4)

t , and D_{sv}
otion of the

nt of tracer
ed bed and
and initial

conditions gives

$$\frac{C_s(\text{at exit})}{C_s(\text{at } t=\infty)} = f\left(\frac{D_{sv}}{u_{s,\text{up}} \pi_f}, \frac{t}{t_s}\right) \quad (5)$$

For a pulse of tracer introduced into a bed with no throughflow of solids,

$$\frac{C_s(t)}{C_s \text{ if well mixed in the bed}} = f\left(\frac{D_{sv} t}{L_f^2}, \frac{z}{L_f}\right) \quad (6)$$

Verloop et al. [16] gave several solutions to Eq. (5) for solids throughflow, and also told where additional solutions may be found. For the batch situation, May [4] gave the solution for one initial condition. Others can be extracted from Carslaw and Jaeger [17].

As understanding of the hydrodynamics of fluidized beds grew, attempts were made to relate the dispersion model to more mechanistic models so that more fundamental measurements could be used for the design of large-scale units. We now look at some of these developments.

Counterflow Solid Circulation Models

In the bubbling bed models sketched in Fig. 6.12, we see some solids flowing up the bed and others flowing down the bed. This upflow and downflow with an interchange between streams is the basis for various counterflow models that have been proposed to account for the vertical mixing of solids.

The simplest version, introduced by van Deemter [18], divides the solids into two streams: one flowing up at a velocity u_{su} , the other flowing down at u_{sd} , with f_u and f_d ($= m^3 \text{ solids/m}^3 \text{ bed}$) being the bed fractions consisting of these streams (see Fig. 2). Consider the movement of some labeled or tagged

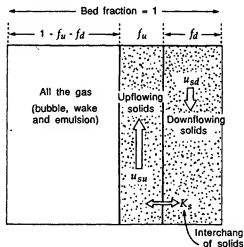


FIGURE 2
Counterflow solid circulation model for the vertical movement of solid in a bubbling fluidized bed.

solids that constitute a fraction X_{su} and X_{sd} ($= m^3$ tagged solids/ m^3 total solid stream) of the up- and downflowing streams. The differential equation describing the vertical movement of these tagged solids and their interchange is then

$$f_d \frac{\partial C_{sd}}{\partial t} + f_d u_{sd} \frac{\partial C_{sd}}{\partial z} + K_s (C_{sd} - C_{su}) = 0 \quad (7)$$

and

$$f_u \frac{\partial C_{su}}{\partial t} + f_u u_{su} \frac{\partial C_{su}}{\partial z} + K_s (C_{su} - C_{sd}) = 0 \quad (8)$$

where the solids interchange coefficient K_s (m^3 tracer/ m^3 bed·s) represents the transfer of tagged solid from one stream to the other.

For a tall enough bed of fine particles and sufficiently large values of elapsed time, van Deemter showed that the changes in concentration of labeled solids could be represented by an effective dispersion coefficient given by

$$D_{sv} = \frac{f_d^2 u_{sd}^2}{K_s (f_d + f_u)} = \frac{f_d^2 u_{sd}^2}{K_s (1 - \delta)(1 - e_f)}, \quad [m^2/s] \quad (9)$$

He then applied this relationship to the data on vertical mixing of silica sand ($u_{mf} = 0.15$ cm/s) reported by de Groot [10], and found values of D_{sv} ranging from 0.03 to 0.23 m^2/s .

Relating the Counterflow to the Dispersion Model

Kunii et al. [19] proposed using the Davidson bubble plus wake as the basis for developing an expression for the interchange coefficient between up- and downflowing solids in beds of fast-rising, hence clouded, bubbles.

Consider the movement of solids around a clouded bubble as shown in Fig. 3. Since the circulation of cloud gas is rapid, Kunii et al. assumed that all the solids from the lower part of the cloud are swept into the wake, mix with the

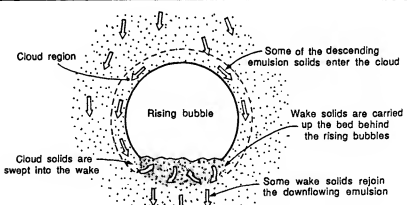


FIGURE 3
Model for the mechanism of interchange of solids between downflowing emulsion solids and upflowing wake solids; from Kunii et al. [19].

solids already there, and eventually leak back into the emulsion. By this process, slowly downflowing emulsion solids are swept into the rising bubble wake and then return to the downflowing emulsion. From this mechanism the interchange coefficient for solids in beds with clouded bubbles is

$$(7) \quad K_s = \frac{(\text{volume of solids transferred from the emulsion to the wake})}{(\text{volume of bubble})(\text{time})}$$

$$= \frac{3(1 - \epsilon_{mf})}{(1 - \delta)\epsilon_{mf}} \frac{u_{mf}}{d_b}, \quad [\text{s}^{-1}] \quad (10)$$

With a somewhat similar model, Chiba and Kobayashi [20] derived the following expression for the interchange coefficient:

$$(8) \quad K_s = \frac{3}{2} \left(\frac{f_w}{1 + f_w} \right) \frac{u_{mf}}{\epsilon_{mf} d_b} \quad (11)$$

Introducing K_s from Eq. (10) into Eq. (9) and simplifying leads to the following expression for the vertical dispersion coefficient in terms of measurable bubble and bed properties:

$$D_{sv} \cong \frac{f_w^2 \epsilon_{mf} \delta d_b u_b^2}{3 u_{mf}} \quad (12)$$

Potter [2] developed a similar expression with the term $1 - \delta$ multiplied on the right-hand side, and with u_o in place of u_b .

As mentioned, van Deemter [18] extracted values of D_{sv} from the experimental results reported by de Groot [10]. Example 1 compares the predictions of Eq. (12) with these reported D_{sv} values. By estimating appropriate values of the bubble rise velocity, one obtains a good fit. In particular, Eq. (12) predicts that D_{sv} should be larger for beds of smaller particles. This is consistent with experimental findings.

Coarse Particle Beds

So far we have only considered the movement of fine solids in tall beds, thus beds with small equilibrium bubbles. When coarse particles are fluidized in beds of aspect ratio of unity, or shallower still, the application of the dispersion model to vertical mixing is not justified unless internals are positioned exactly uniformly across the bed, in which case the spacing of the internals governs the scale of solid mixing.

Such positioning is not really practical; hence one may find a thick stream of solids descending at vessel walls or in the spaces between neighboring tube banks. Saitai [14] proposed another counterflow model, which accounts for this third phase of solids that descends along these walls. This model is sketched in Fig. 4. On fitting his model to tracer data from a $1.2 \text{ m} \times 1.2 \text{ m}$ tube-filled bed, he gave the mean velocity of descending solids as $1.7\text{--}1.8 \text{ cm/s}$ in the main part of the bed and $4.8\text{--}5.8 \text{ cm/s}$ along the wall for $u_o = 0.6\text{--}0.9 \text{ m/s}$ and $u_{mf} = 0.3 \text{ m/s}$. Van Deemter [3] surveyed these counterflow solid circulation models.

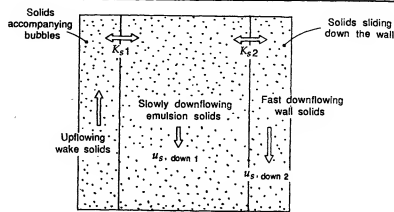


FIGURE 4

Three-region counterflow model for vertical solid movement in large particle shallow beds with internals; from Sitnai [14].

EXAMPLE 1

Vertical Movement of Solids

Calculate the vertical dispersion coefficient from Eqs. (3) and (12) and compare these values with the values extracted by van Deemter [18] from the experiments of de Groot [10] in various sized vessels.

Data $u_{mf} = 0.015 \text{ m/s}$, $\epsilon_{mf} = 0.5$, $U_0 = 0.1 \text{ m/s}$, $\delta = 0.2$, $d_b = 0.06 \text{ m}$

$d_t (\text{m})$	0.1	0.3	0.6	1.5
$u_b (\text{m/s})$	0.40	0.75	0.85	1.1
Reported				
$D_{sv} (\text{m}^2/\text{s})$	0.030	0.11	0.14	0.23

SOLUTION

Using Eq. (3) we find

$$D_{sv} = 12(10)^{0.5} d_t^{0.9} = 38 d_t^{0.9}, \quad [\text{cm}^2/\text{s}]$$

The main problem in using Eq. (12) is choosing a reliable value for the wake fraction f_w . Hamilton et al. [21] report $f_w = 1-2.9$ for this range of particle size (mean value of 2), whereas Fig. 5.8 gives $f_w = 0.32$. Although not very satisfactory, we average these f_w values. Thus

$$f_w = \frac{0.32 + 2}{2} = 1.16 \approx 1.2$$

Then Eq. (12) becomes

$$D_{sv} = \frac{(1.2)^2 (0.5)(0.2)(0.06) U_0^2}{3(0.015)} = 0.192 U_0^2$$

Thus we find

d_t	0.1	0.3	0.6	1.5 m
D_{sv} , from experiment	0.030	0.11	0.14	$0.23 \text{ m}^2/\text{s}$
D_{sv} , from Eq. (3)	0.030	0.08	0.15	$0.35 \text{ m}^2/\text{s}$
D_{sv} , from Eq. (12)	0.031	0.11	0.14	$0.23 \text{ m}^2/\text{s}$

Horizontal Movement of Solids

Experimental Findings

The horizontal movement of solids was first studied by Brötz [22] in a shallow rectangular bed, as shown in Fig. 5. Measuring the rate of approach to uniformity after removal of the dividing plate then gave the information needed to evaluate the horizontal dispersion coefficient D_{sh} . A similar approach was used by other investigators [23-25].

Heertjes et al. [26] suggested that the wake material scattered into the freeboard by the bursting bubbles could contribute significantly to the horizontal movement of solids. Hirama et al. [24] and Shi and Gu [27] used partition plates in the freeboard just above the bed to study this effect.

All of these investigators used rather shallow beds of height between 5 and 35 cm. In contrast, Bellgardt and Werther [28] made measurements in a much larger bed, namely a $2\text{ m} \times 0.3\text{ m}$ bed about 1 m deep. Quartz sand ($d_p = 450\text{ }\mu\text{m}$) was fluidized, and careful measurements confirmed that vertical mixing was much faster than horizontal mixing, thus justifying the use of a one-dimensional dispersion model in the horizontal direction. They found $D_{sh} = 6-25\text{ cm}^2/\text{s}$ for $r_o = 0.23-0.73\text{ m/s}$. Applying their model to coal combustion and gasification, Bellgardt et al. [29] presented a performance model for solid movement that was tested in TVA's 20-MW FBC pilot plant.

Table 1 gives information on the reported studies of horizontal movement of solids. We summarize these findings as follows:

- Comparing the dispersion coefficient for the horizontal movement with the vertical movement of solids (compare Table 1 with Fig. 1), we see that D_{sh} is roughly an order of magnitude smaller than D_{sv} .
- D_{sh} increases with bed width. For example, Hirama et al. [24] in their very small units found a 60% increase for a doubling in bed width.
- The scattering of solids into the freeboard contributes significantly to D_{sh} in shallow beds.

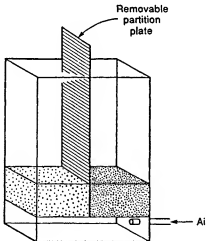


FIGURE 5
Experimental setup used by Brötz [22] to study the horizontal movement of solids.

TABLE 1 Range of Experimental Data for the Horizontal Movement of Solid

Investigators	Bed (m)	Particles
Mori and Nakamura [23] (1965)	0.9 × 0.3	Polyvinyl chloride
Hirama et al. [24] (1975)	0.4 × (0.042, 0.08, 0.2)	Glass beads, cracking cat.
Bellgardt and Werther [28] (1984)	2.0 × 0.3 $L_f \approx 1$	Quartz sand
Kato et al. [30] (1985)	0.5 × 0.2 Vertical tubes 0.032 Horizontal tubes 0.018	Activated carbon
Shi and Gu [27] (1986)	0.57 × 0.05	Resin, silica gel

- Vertical and horizontal internals reduce D_{sh} significantly. From Kato et al. [30] we find this effect to be as follows:

No tubes present	<i>d_{te}</i> (cm)	Effective bed diameter with tubes present, <i>d_{te}</i> (cm)				
		15.9	10.6	7	5	~2.6
D_{sh} (cm ² /s) with vertical tubes	20	—	10	—	6	3
D_{sh} (cm ² /s) with horizontal tubes	20	8	—	6	—	3

This table shows no appreciable difference between the effect of horizontal and vertical tubes. Kato et al. [30] also found that for their operating conditions D_{sh} was unaffected by bed height.

Mechanistic Model Based on the Davidson Bubble

Consider the following mechanism for the horizontal movement of solids in a fine particle bed of fast rising bubbles, as sketched in Fig. 6.

Postulate. As a bubble rises, it pushes emulsion aside. However, the solids passing close to the bubble enter its cloud and are then drawn into the wake, whose diameter is roughly α times the bubble diameter. Solids mix uniformly in the wake and leave the wake from random positions, thereby giving rise to horizontal mixing. Solids further from the bubble move aside as the bubble passes, but return close to their original position.

For this mechanism it is simplest to evaluate the horizontal dispersion coefficient D_{sh} in terms of the Einstein random walk equation:

$$D_{sh} = \frac{(\text{fraction of solids that mix})(\text{mean square distance moved})}{4(\text{time interval considered})}$$

$$= \frac{1}{4} \left(\frac{\text{fraction of bed solids that enter bubble wakes}}{\text{to mix there per unit time}} \right) \Delta r^2 \quad (13)$$

ment of Solid
es
yl
e
beads,
ng cat.
sand
ed
el

om Kato et al.

ith

5 ~2.6

5 3

— 3

horizontal and
conditions D_{sh}

of solids in a

However, the
rawn into the
r. Solids mix
hereby giving
aside as the

tal dispersion

(13)

Particles		
d_p (μm)	u_{mf} (m/s)	D_{sh} (m^2/s) at u_0 (m/s) and d_b (m)
595	0.295	$1-7 \times 10^{-3}$ at $u_0 = 0.4-0.7$
150, 460	0.024, 0.15	$0.7-2 \times 10^{-3}$ at $u_b d_b = 1-2 \times 10^{-2}$
75	0.0055	$0.6-3 \times 10^{-3}$ at $u_b d_b = 1-6 \times 10^{-2}$
		$d_b = 0.02-0.06$ at $u_o - u_{mf} = 0.05-0.4$
450	0.17	$0.6-2.5 \times 10^{-3}$ at $u_o - u_{mf} = 0-0.5$
394-1073	0.035-0.27	$0.1-1 \times 10^{-3}$ at $u_o - u_{mf} = 0.1-0.6$
		$0.2-1 \times 10^{-3}$ at $u_o - u_{mf} = 0.15-0.6$
450, 750	0.076, 0.20	$d_e = 0.026-0.159$
620	0.0905	$-0.3-0.8 \times 10^{-3}$ at $L_{mf} = 0.02-0.07$

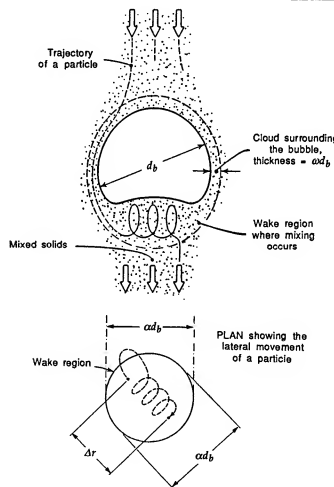


FIGURE 6
The horizontal movement of solids according to the model of Kunii and Levenspiel [31].

Kunii and Levenspiel [31] evaluated the terms of this expression. Thus for clouded Davidson bubbles the term in parentheses depends on bubble size, cloud thickness, and bubble density in the bed. Next, from probability theory the mean square horizontal shift of a particle on passing through the bubble wake is given by

$$\overline{\Delta r^2} = \frac{(\alpha d_b)^2}{4}$$

where αd_b is the effective diameter of the wake.

Replacing all quantities into Eq. (13) gives, in general, for both fast and intermediate bubbles,

$$D_{sh} = \frac{3}{16} \frac{\delta}{1-\delta} \alpha^2 d_b u_{br} \left[\left(\frac{u_{br} + 2u_f}{u_{br} - u_f} \right)^{1/3} - 1 \right] \quad (14)$$

For fast bubbles with thin clouds typical of fine particle systems, or $u_{br} \gg u_f$, Eq. (14) simplifies to

$$D_{sh} = \frac{3}{16} \frac{\delta}{1-\delta} \frac{\alpha^2 u_{mf} d_b}{\epsilon_{mf}} \quad (15)$$

For fine Geldart A and AB solids ($d_p = 60$ and $150 \mu\text{m}$), Kunii and Levenspiel found that Eq. (15) with $\alpha = 1$ fitted their data, while for larger Geldart BD solids (quartz, $d_p = 450 \mu\text{m}$), Bellgardt and Werther [28] found that $\alpha = 0.77$ well represented their data.

Equations (14) and (15) do not account for the scattering of solids at the bed surface, and Shi and Gu [27] presented a model that does account for it. However, since this freeboard scattering is restricted to the top layer of bed solids, its effect on D_{sh} for the bed as a whole becomes smaller for deeper beds.

Equation (15) can be used for approximate prediction of D_{sh} for deep beds, but more importantly it suggests how changes in system variables such as u_{mf} , u_o , and d_b will affect D_{sh} . Example 2 concerns D_{sh} .

EXAMPLE 2

Horizontal

Drift of

Solids

Bellgardt and Werther [28] presented the following data on the horizontal dispersion coefficient for quartz solids in fluidized beds. Compare the predicted D_{sh} from Eq. (14) or (15) with their findings.

Data

Bed size: $0.3 \times 2 \text{ m}$, $L_{mf} = 0.83 \text{ m}$

Quartz sand: $d_p = 450 \mu\text{m}$, $\epsilon_{mf} = 0.42$, $u_{mf} = 0.17 \text{ m/s}$

$u_o (\text{m/s})$	0.37	0.47	0.57	0.67
Reported $D_{sh} (\text{m}^2/\text{s})$	0.0012	0.0018	0.0021	0.0025

From Fig. 6.10(a) we estimate $d_b = 0.10\text{--}0.14 \text{ m}$ for this range of gas velocities.

SOLUTION

Let us show the solution for the first data point, $u_o = 0.37 \text{ m/s}$, and for the smallest estimated bubble size, $d_b = 0.10 \text{ m}$. Then the first problem is to decide whether to

Thus for
bble size,
ity theory
the bubble

h fast and

(14)

$u_{br} \gg u_f$,

(15)

Levenspiel
eldart BD
= 0.77 well

solids at the
ount for it.
er of bed
eeper beds.
h for deep
oles such as

al dispersion
 D_{sh} from Eq.

s velocities.

the smallest
e whether to

use Eq. (14) or (15). For this determine whether $u_{br} \gg u_f$. Now

$$\begin{aligned} u_{br} &= 0.711(d_b g)^{1/2} = 0.711(0.1 \times 9.8)^{1/2} = 0.70 \text{ m/s} \\ u_b &= u_o - u_{mf} + u_{br} = 0.37 - 0.17 + 0.70 = 0.90 \text{ m/s} \\ u_f &= \frac{u_{mf}}{\epsilon_{mf}} = \frac{0.17}{0.42} = 0.40 \text{ m/s} \end{aligned}$$

Since we do not have $u_b \gg u_f$, we use Eq. (14) instead of Eq. (15) to calculate D_{sh} . In addition, since we are not dealing with fine Geldart A or AB solids, we take $\alpha = 0.77$ in this equation (see just after Eq. (15)).

The last quantity needed before using Eq. (14) is δ . Since u_{br} is close to u_f , we use Eq. (6.27) to give

$$\delta \cong \frac{u_o - u_{mf}}{u_b + u_{mf}} = \frac{0.37 - 0.17}{0.90 + 0.17} = 0.187$$

Substituting all into Eq. (14) gives

$$D_{sh} = \frac{3}{16} \frac{0.187}{1 - 0.187} (0.77)^2 (0.1)(0.70) \left[\left(\frac{0.70 + 2 \times 0.40}{0.70 - 0.40} \right)^{1/3} - 1 \right] = 0.0013 \text{ m}^2/\text{s}$$

Similar calculations are made for other u_o values. The final results and comparison with the experimental values gives

u_o	0.37	0.47	0.57	0.67 m/s
D_{sv} calculated (at $d_b = 0.10 \text{ m}$)	1.3	1.9	2.5	$3.2 \times 10^{-3} \text{ m}^2/\text{s}$
D_{sv} calculated (at $d_b = 0.14 \text{ m}$)	1.4	2.2	2.9	$3.6 \times 10^{-3} \text{ m}^2/\text{s}$
D_{sv} from experiment	1.2	1.8	2.1	$2.5 \times 10^{-3} \text{ m}^2/\text{s}$

The calculated values are somewhat high.

Segregation of Particles

Numerous processes require fluidizing a mixture of solids of very different density. As an example, in one step in the production of titanium or zirconium a mixture of the metal oxide (high-density solid) and coke (very low density) is fluidized by chlorine gas at high temperature. To achieve close to 100% conversion of chlorine, bed bubbling should not be too vigorous; hence the gas velocity should not be too high. On the other hand, the gas velocity should not be too low or solids will separate out. What size ratio of solids and what gas velocity should be used in such situations? The whole question of the mixing-segregation equilibrium is of vital concern in these situations.

Mixing-Segregation Equilibrium

Much has been reported in recent years on the mixing-segregation phenomenon in gas fluidized beds, especially on binary systems of different size and/or density; see [32]. Here, particle segregation occurs at close to u_{mf} of the biggest or heaviest particles in the bed. Also, this whole question mainly concerns large particle systems.

Cooperative investigations on particle segregation were carried out by Rowe et al. [33,34], Nienow et al. [35,36], Chiba [37–39] and others, in which the following special terminology was used for the fluidized bed components:

jetsam: component that ultimately sinks

flotsam: component that floats to the top of the bed

We summarize those findings as follows:

With solids of the same size but different density, the bed segregates readily. When this occurs, the dense material forms a relatively pure bottom layer. The upper layer always contains some of the denser solids, more or less uniformly dispersed.

Particles of different size but the same density will also segregate, but not easily. Even particles an order of magnitude different in diameter will mix fairly uniformly at moderate bubbling conditions. With a wide size distribution of particles rather than a sharp cut of two distinct sizes, we may expect much less segregation.

When the gas velocity is close to u_{mf} , the segregation of the jetsam can be severe. At higher gas velocities it is less severe. Figure 7 illustrates the segregation pattern in binary mixtures; Fig. 8 illustrates this behavior for mixtures of commercial powders. Thus, Fig. 8(a) shows a sharp segregation of denser material (density ratio = 1.8:1), and Fig. 8(b) shows that even with very different particle sizes (size ratio = 3.5:1) segregation is minor. Both systems display less segregation when the gas velocity is raised.

Rowe et al. [33] proposed using a solids mixing index defined as

$$M = \left(\frac{\text{fraction of jetsam in the top portion of the bed}}{\text{fraction in a well-mixed bed}} \right) = \frac{X_{sj, \text{top}}}{\bar{X}_{sj}} \quad (16)$$

$M = 0$ and 1 correspond to complete segregation and complete mixing, respectively.

Noting that the jetsam fraction in Fig. 8 is practically constant in a large portion of the bed, we can use this value to get an approximation for M ; thus

$$M \approx \frac{X_{sj, \text{straight-line portion}}}{\bar{X}_{sj}} \quad (17)$$

Factors affecting particle segregation were studied by Rowe and Nienow [34,35] in terms of this index.

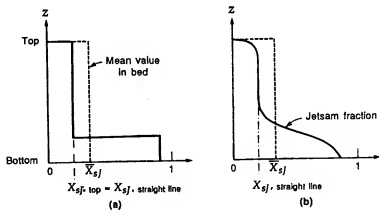


FIGURE 7

Distribution of solids in strongly segregating binary mixtures: (a) idealized segregation at low fluidizing velocity; (b) pattern of segregation at vigorous bubbling conditions.

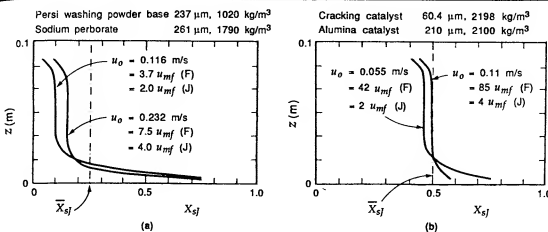


FIGURE 8
Vertical segregation of commercial solids; $d_i = 0.141 \text{ m}$, $L_m = 0.1\text{--}0.15 \text{ m}$; adapted from Rowe et al [33]; (a) different density materials; (b) different sized materials.

Rowe et al. [33] were the first to suggest that rising bubbles are the vehicle for particle segregation. Thus, all solids, both flotsam and jetsam, are carried up the bed in the bubble wakes. However, only the larger denser particles preferentially move down the bed as a bubble passes by. They emphasized that this upflow in the bubble wake is the only way that the smaller less dense particles can reach the top of the bed.

Mathematical models to account for the axial distribution of solids at a stable mixing-segregation equilibrium have been proposed by several research groups. Chiba et al. [39] reviewed and summarized these works. They also explained the preferential downflow of denser solids as follows: the denser larger particles tend to fall preferentially through the temporarily disturbed region (the wake) behind the bubbles. This downward movement of jetsam is clearly analogous to the jiggling separation technique.

Chiba et al. [38] found that an increase in pressure promoted solid mixing, and explained this in terms of increased wake fractions. This observation suggests that for their system the mixing of bed solids by the upflow of wakes was more important than the preferential downflow of jetsam from the wakes.

Steady State Separation of Particles

A number of operations are being explored that require fluidization with separation of two different kinds of solids: for example, driers in which fine wet solids are mixed with a hot solid heat carrier, and some advanced combustor-gasifiers that fluidize dolomite and char. Some researchers [35,40-43] have studied these systems.

Note that with one inflow and one outflow stream for a mixture of solids that readily segregate, the bed composition will adjust itself so that at steady state the outflow composition will equal the inflow. Of course, the location of the outflow will influence the bed composition. Figure 9 illustrates this. With two outflow streams, one should be able to get a good separation of components, and Chiba et al. [36] showed how to predict the composition of the two outflow